Published in final edited form as:
Stem Cells. 2014 March ; 32(3): 791–801. doi:10.1002/stem.1598.

Stress hematopoiesis is regulated by the Krüppel-like transcription factor ZBP-89

Xiangen Li[a], **Rachael D Romain**[b], **Dongsu Park**[c,d], **David T. Scadden**[c,d], **Juanita L. Merchant**[b], and **M. Amin Arnaout**[a,d]

[a]Leukocyte Biology & Inflammation Program, Division of Nephrology, Massachusetts General Hospital, Charlestown, MA

[b]Division of Gastroenterology, University of Michigan, Ann Arbor, MI

[c]Center For Regenerative Medicine, Massachusetts General Hospital, Boston, MA

[d]Harvard Stem Cell Institute, Cambridge, Massachusetts

Abstract

Previous studies have shown that ZBP-89 (Zfp148) plays a critical role in erythroid lineage development, with its loss at the embryonic stage causing lethal anemia and thrombocytopenia. Its role in adult hematopoiesis has not been described. We now show that conditional deletion of ZBP-89 in adult mouse hematopoietic stem/progenitor cells (HSPC) causes anemia and thrombocytopenia that are transient in the steady state, but readily uncovered following chemically induced erythro/megakaryopoietic stress. Unexpectedly, stress induced by bone marrow transplantation of *ZBP89*$^{-/-}$ HSPC also resulted in a myeloid-to-B lymphoid lineage switch in bone marrow recipients. The erythroid and myeloid/B lymphoid lineage anomalies in *ZBP89*$^{-/-}$ HSPC are reproduced *in vitro* in the *ZBP-89*-silenced multipotent hematopoietic cell line FDCP-Mix A4, and are associated with the upregulation of *PU.1* and downregulation of *SCL/Tal1* and *GATA-1* in ZBP89-deficient cells. Chromatin immunoprecipitation and luciferase reporter assays show that ZBP-89 is a direct repressor of *PU.1* and activator of *SCL/Tal1* and *GATA-1*. These data identify an important role for ZBP-89 in regulating stress hematopoiesis in adult mouse bone marrow.

Keywords

Stress hematopoiesis; hematopoietic stem cells; erythroid progenitors; transcription factors; transplantation

Introduction

The hematopoietic system originates from a small population of self-renewing hematopoietic stem cells that differentiate into the various erythroid, myeloid and lymphoid lineages. The hematopoietic lineages tend to be specified in a stepwise process of binary decisions, dependent on particular genetic programs under control of transcription factors.

Correspondence to: M. Amin Arnaout, Leukocyte Biology & Inflammation Program, Division of Nephrology, Massachusetts General Hospital, Charlestown, MA, 02129, Tel: 617-726-5663, Fax: 617-726-5671. aarnaout1@partners.org.

Author contributions. MAA conceived and designed experiments; XL, DP, JLM performed experiments; MAA and DTS analyzed data; MAA wrote the paper.

Disclosure of potential conflicts of interest. The authors indicate no potential conflicts of interest.

See www.StemCells.com for supporting information available online.

The lineage-specifying and autoregulatory factors PU.1 and GATA1 form a master genetic switch that is responsible for determining the myeloid/lymphoid and erythroid lineages [1, 2], respectively, commonly acting in concert with lineage-restricted factors such as SCL/TAL1 [3, 4] and CCAAT/enhancer binding protein α (C/EBPα)[5]. PU.1 and GATA1 mutually inhibit each other's expression and transactivation functions, thus favoring one lineage fate over the other [6].

ZBP-89 (Zfp148) belongs to a novel class of GC-rich binding transcription factors phylogenetically conserved in mammals, which contain a characteristic array of four Krüppel type zinc fingers [7]. Zebrafish ZBP-89 morphants [8] and ZBP-89 knockout mice [9] die at the embryonic stage with severe anemia and thrombocytopenia. The role of ZBP-89 in adult hematopoiesis has not been explored.

To investigate its role in adult hematopoiesis, we conditionally deleted *ZBP-89* in mouse hematopoietic stem/progenitor cells (HSPC). We observed an early drop in red blood cell (RBC) and platelet (PLT) counts in peripheral blood (PB), and a significant reduction in the number of megakaryocyte/erythrocyte progenitors (MEP) in *ZBP-89*-deficient bone marrow (BM). The defect in the erythro-megakaryocytic lineage was, however, transient under steady state conditions, but was readily uncovered by chemical induction of hematopoietic stress. An unexpected reduction in the myeloid lineage and an increase in B lymphoid lineage were observed in *ZBP89*$^{-/-}$ BM recipients. Transcriptional profiling revealed a significant increase in *PU.1* and a reduction in *SCL and GATA1* transcripts in HSPC. Similar anomalous hematopoietic lineage and transcriptional profiles were observed *in vitro* when ZBP-89 was stably-silenced in the nonleukemic multipotent progenitor cell line FDCP-Mix A4 (A4) [10]. Chromatin immunoprecipitation (ChIP) and luciferase reporter assays showed that ZBP-89 binds to the *PU.1*, *SCL* and *GATA1* promoters, repressing *PU.1* and activating *SCL* and *GATA1*. The significance of these findings is discussed.

Material and Methods

Mice and cell lines

Mice expressing the targeted *ZBP-89* locus with flanking LoxP sites (*ZBP-89*$^{fl/fl}$) were produced as described [11]. Conditional deletion of *ZBP-89* in the hematopoietic system of mice (C57BL/6-CD45.2^{+} background) was generated as shown in Figure 1A. Transgenic mice expressing an interferon-inducible Cre recombinase (*Mx*^{Cre}) (Kuhn et al, 1995) were kindly provided by Dr. Hanno Hock (MGH Cancer Center). Murine erythroleukemia cell line MEL and the non-hematopoietic QM7 cell line, which lacks endogenous ZBP-89 [12], were obtained from ATCC and maintained in DMEM medium containing 10% fetal calf serum. The multipotent A4 cell line was maintained in Iscove's modified Dulbecco's Medium (IMDM) supplemented with 20% horse serum and Interleukin-3 (IL-3)(100 units/ml, R&D Systems). Congenic C57BL/6-CD45.1 mice (6 to10 weeks old) were used as donors for purification of wild type cells and as recipients for BM transplantation (BMT) experiments. All animal experiments were performed in accordance with legal and ethical requirements demanded by law and approved by the Massachusetts General Hospital Subcommittee on Research Animal Care.

ZBP-89-silenced MEL and A4 cells

21-mers encoding 5 different short hairpin (sh) RNAs (H2 to H6)(Broad Institute, Cambridge, MA) were used for stable silencing of mouse wild-type *ZBP-89* in MEL cells. Each shRNA was cloned into the pLK0.1-puromycin plasmid and the plasmid incorporated into lentivirus using the helper and packaging system pΔD8.9, pMD.G (VSV-G). Virus-infected MEL cells were selected by puromycin (5μg/ml), isolated and tested for ZBP-89

silencing by Real-time reverse-transcribed polymerase chain reaction (RT-PCR) and western blotting. The H5 21-mer, which produced maximal silencing of ZBP-89 in MEL (Supplemental Figure 1), was used to stably silence ZBP-89 in A4 cells.

Induction of the *Cre* transgene *in vivo*

To induce the Mx^{Cre} transgene, *ZBP-89*$^{fl/fl}$-Mx^{Cre+} or *ZBP-89*$^{fl/fl}$-Mx^{Cre-} control mice were injected intraperitoneally with polyinosinic-polycytidylic acid (pIpC, Amersham) at 20 μg/g dissolved in saline on every other day for a total of seven doses. Mouse PB and bone marrow cells were harvested for analysis at different time points after the last pIpC injection.

Recombination analysis

PCR analysis was performed using progenitor colony genomic DNA. To amplify the floxed (non-deleted) allele product and flanking DNA sequence, the forward/reverse primers *F1*, 5′-AGACCTACGACCCACAGGGTGG-3; *R1*, 5′-GGCTT CTCTCCACTGTGAGTT-3′; *F2*, 5′-TGTCCTCTCACCTCTGCACATTCAGCGACAC-3′ (between intron 7 and the reverse primer); *R2*, 5′-TGCGCCACAGACACACATC AGTCTTCAGATCG-3′ (at the 3′ untranslated region) were used. To amplify the recombined allele product and *Cre* gene, the following primers were used: *MH61*, 5′-GACCAGGTTCGTTCACTCATGG-3′; *MH63*, 5′-AGGCTAAGTGCCTTCTCTACAC-3′. The internal control primers were: *IMR0042*, 5′-CTAGGCCACAGAATTGAAAGATCT-3′ and *IMR0043*, 5′-GTAGGTGGAAATTCTAGCATCATCC-3′.

Hematologic analysis and cell culture

Blood samples were obtained from mice by tail puncture and placed in EDTA-coated microtubes. Blood counts were performed with a VetScan HM5 (Abaxis Veterinary Diagnostic Company). Murine colony assays were performed by plating 1×10^5 BM cells/ml of methocult M3434 (Stem Cell Technologies, Vancouver, BC) in 6-well plates in duplicate and cultured at 37°C for 10 days. Burst-forming unit erythroid (BFU-E), CFU-granulocyte (CFU-G), CFU-granulocyte-macrophage (CFU-GM), granulocyte-erythrocyte-macrophage-megakaryocyte (CFU-GEMM) colony numbers were counted based on colony morphology.

Chemical induction of hemolytic anemia and thrombocytopenia

One week post pIpC, mice were injected subcutaneously with 0.4% phenylhydrazine (PHZ; Sigma-Aldrich) in saline (12μl/g body weight) for 2 consecutive days. Mouse peripheral blood was collected for analysis on day 5 and day 15 after PHZ injection. Bone marrow and spleen cells were harvested from control and *ZBP-89* CKO mice (n=3 in each group) on day 5 post PHZ injection. To induce thrombocytopenia, mice were injected intraperitoneally with 150 mg/kg 5-fluorouracil (5FU)(Sigma, St Louis, MO) one week post pIpC, and samples were collected 6 days later.

Hematologic analysis, flow cytometry and cell sorting

PB cell types were identified by flow cytometry following staining with cell-type specific antibodies using LSR II cytometer (BD Biosciences). Single cell suspensions of spleen and BM cells were obtained as detailed elsewhere [13]. Surface phenotypes of isolated HSPC were as follows: BM-derived Lineage-negative (Lin^-), LSK (Lin^- $Sca\text{-}1^+$ $C\text{-}kit^+$); LT-HSC (LSK $CD150^+CD48^-$); multipotent progenitors (MPP) (LSK $CD34^+FLK3^+$); common myeloid progenitors (CMP) ($Lin^-C\text{-}kit^+Sca1^-CD34^{med}$ $CD16/32^{med}$); common lymphoid progenitors (CLP) ($Lin^-C\text{-}kit^{med}$ $Sca1^{med}IL7R^+$); granule-monocyte progenitors (GMP) ($Lin^-C\text{-}kit^+$ $Sca1^-CD34^+CD16/32^+$); MEP ($Lin^-C\text{-}kit^+Sca1^-CD34^-CD16/32^-$); precursor-B-progenitor B (Pre-Pro-B) ($AA4.1^+IL\text{-}7R^+B220^{Med}C\text{-}kit^+$); Pro-B ($AA4.1^+IL\text{-}7^+B220^{Med}C\text{-}kit^-$); Pre-B ($AA4.1^+IL\text{-}7^+B220^{hi}C\text{-}kit^-$); BM- or spleen-derived

Pro- ($CD71^{high}Ter119^{low}$), Basophilic- ($CD71^{high}Ter119^{high}$), polychromatic ($CD71^{low}Ter119^{high}$) erythroblasts [14]. Quantitative analysis of the distinct stages of erythroblast development was conducted as described [15]. Briefly, bone marrow or spleen cells were first blocked with rat anti-mouse CD16/32 (BD Science) for 15 minutes, stained with the labeled rat anti-mouse antibodies FITC-ter119, APC-CD44, APC-Cy7 CD45, APC-Cy7 CD11b and APC-Cy7 GR1 (BD sciences), then subsequently stained with 7-AAD (BD science) before cell analysis using flow cytometry. In chimeric mice, PB and HSPC were stained with both Pacific blue-anti-CD45.2, PE-Cy7-anti-CD45.1 and the lineage specific FITC-anti-CD41, PE-anti-CD11b, PE-CY5-anti-CD3 and APC-anti-B220 antibodies, and the dual-positive (Pacific blue-$CD45.2^+$ and lineage-specific cell populations) were gated and quantified. Wild-type or *ZBP-89*-silenced A4 cells at various passages (12–24 weeks) were immunostained after 1 week in culture with mAbs to the lineage-specific markers CD41, CD11b, CD3 and B220 followed by flow cytometry.

Total RNA isolation and RT-PCR

Total RNA was extracted from fractionated BM progenitors or from A4 cells with the RNAqueous-4PCR kit (AMBION INC, Austin, TX). For each experiment, BM progenitor-derived RNAs from two *ZBP-89* CKO or two control mice were pooled. Reverse transcription of BM progenitor- or A4-derived RNA was performed with the High Capacity cDNA Reverse Transcription Kit (AB applied Biosynthesis). RT-PCR was run on Stratagene300 (Stratagene) using Brilliant SYBR Green QPCR Master Mix (Stratagene). Sequences for the primers used are as follows. ZBP89 *RTF*, 5′-CGGCATAGACGAAATGCAGTC-3′; ZBP89 *RTR*, 5′-CCTGGTGAGGCAAACTTCGAT-3′; *SCL*RTF, 5′-CACTAGGCAGTGGGTTCTTTG-3′, *SCL* RTR, 5′-GGTGTGAGGACCATCA GAAATCT-3′; *GAPDH* RFF,5′-AGGTCGGTGTGAACGGATTTG-3′; *GAPDH* RTR,5′-TGTAGACCATGT AGTTGAGGTCA-3′; GATA1RTF, 5′-TGGGGACCTCAGAACCCTTG-3′; *GATA1* RTR, 5′-GGCTGCATTTGGGGAAGTG-3′; *PU.1*RTF,5′-GGACATGGTGTGC GGAGAA-3′, *PU.1* RTR, 5′-AGAAAGCCATAGCGATCACTACT-3′; TIF1γ RTF, 5′-AGATAATGCAAGTGCAGTTGGT-3′, TIF1γRTR, 5′-ACGTCAATCTATCACACGTTTCA-3′;C/EBPα RTF,5′-AGGACACGGGGACCATTAG-3′; C/EBPα RTR,5′-TAGACGTGCA CACTGCCATT-3′; *FOXO1* RTF, 5′-ATGCTCAATCCAGAGGGAGG-3′; *FOXO1* RTR, 5′-ACTCGCAGGCCACTTAGAAAA-3′; *Gfi1* RTF, 5′-CCCTTTGCGTGCGAGATGT-3′, Gfi1RTR, 5′-CACTGCCTTGTGTTGCTCCA-3′; *C-myb* RTF, 5′-CAGAAGAGGAGGACA GAATCATTT; *C-myb* RTR, 5′-TTCCAGTGGTTCTTGATAGCATTA-3′; *FOG1* RTF, 5′-CAGAGCCTTATCCCCTGAGAG-3′; *FOG1* RTR, 5′-CGGCTTCTTCAGTTAGGACCT-3′.

Bone marrow repopulation assays

$CD45.2^+$ *ZBP-89*$^{flox/flox}$*-Mx-Cre*$^-$ or *ZBP-89*$^{flox/flox}$*-Mx-Cre*$^+$ bone marrow cells mixed with competitor wild-type CD45.1 bone marrow cells in a 1:1 ratio (a total of 2×10^6 cells) were injected intravenously into the lateral tail vein of congenic age-matched $CD45.1^+$ mouse recipients (n=5 per genotype) that were lethally-irradiated one day before BMT. 6 weeks later, 20 μg/g pIpC were injected into recipient mice every other day (for a total of seven doses), following which PB cells and BM HSPC were harvested at different times and analyzed for expression of CD45.1 and CD45.2 alleles. For secondary BMT, $CD45.2^+$ *ZBP-89*-excised BM cells were harvested from primary recipients 7 months after the last pIpC dose, and 2×10^6 cells were injected into 6-week old irradiated $CD45.1^+$ recipient mice (n=5 per genotype). Reconstitution of secondary recipients was analyzed 6 to 36 weeks after BMT.

Chromatin Immunoprecipitation (ChIP) Assays

This was carried out as described [16]. Briefly, 5×10^6 MEL cells were cross-linked with 1% (v/v) formaldehyde, the reaction stopped with glycine, and washed cells pelleted then resuspended in lysis buffer. Following homogenization, the nuclei were sonicated on ice to a DNA size of 200–800 bp. Protein-DNA complexes were immunoprecipitated using an anti-ZBP-89 antibody (SC-19408; Santa Cruz) (or immunoglobulin G (IgG) as a negative control), and the DNA-protein complexes collected by binding to A/G plus-agarose beads. Washed beads were eluted in 1% SDS/0.1mM $NaCHO_3$. DNA was reverse-crosslinked by incubation at 68°C overnight then purified using QIAGEN quick PCR purification kit. PCR was performed using 10% (3μl) of the bound DNA fraction from the chromatin precipitate or 1% (1μl) of the input DNA fraction. The murine *SCL 1a/b* promoter fragments (−2000 to +1bp) containing the *ZBP-89* element were amplified using the forward primer 5′-TCCCAACGTGAGCGCTCAGCC-3′ and the reverse primer 5′-TGTGCGCCGCCGA GATAAGG-3′ for *1a* region, and the forward primer 5′-TTCCTCCGTCTTTCCCCATGC-3′ and the reverse primer 5′-AGCACTCTCAACCCGGCCGCC-3′ for *1b* region. The murine *PU.1* 3.4 kb HindIII UTR fragments containing the *ZBP-89* element were amplified using the primers F1: 5′-ACCCCGGGGTTGAAGGAACAC-3′, R1; 5′-TCTCCAGAAAGCCTG TTGCTGTCAG-3′; F2, 5′-TAACCCCTGCACATGAAAGCC-3′, and R2, 5′-TCTGGG CAGGGTCAGAGTGCC-3′. The murine 129bp fragment containing the ZBP-89 binding site in G1HE was amplified using the forward primer 5′-TCCCTTATCTATGCCTTCCCA-3′ and the reverse primer 5′-ATGAAGGGTGCCTCTAAGGAC-3′. PCR products were separated in 2.0% agarose gels containing 0.5 μg/ml ethidium bromide.

Site-directed mutagenesis

Mutations in the ZBP-89 binding site of murine SCL *1a* promoter were generated by overlapping PCR, changing the wild type ZBP-89 *Ia* binding site core sequence 5′-cgcttatcgGGGGcggggcc-3′ to 5′-cgcttcgGAAGcGgggcc-3′. PCR reactions were performed using WT forward primer (WTFP): 5′-GGGGTACCTCAGTTAGCGGTGAAGGCTCATG-3′ (tagged KpnI site underlined) and mutant reverse primer: 5′-GGCCCGCCAGCTTCCGATAAGCG-3′, to generate the first fragment, and the mutant forward primer: 5-CGCTTATCGGAAGCTGGCGGGCC-3′, and WT reverse primer (WTRP): 5′-CCGCTCGAGACCCGGCCGCCCGCACACACC-3′ (tagged XhoI site underlined) to generate the second fragment. DNAs from both PCR amplifications were gel extracted and used in overlapping PCR using WTFP and WTRP, and the final product was KpnI/XhoI restricted then inserted into the KpnI/XhoI- digested pGL2 vector. XL1-Blue competent cells were transformed with ligation mix, plated on LB Amp plates, and incubated overnight at 37°C. Colonies were screened and clones confirmed by DNA sequencing. A similar strategy was used in replacing WT ZBP-89 core binding site 5′-ggctccctctCCCCcgtctcttc-3′ in *Ib* with 5′-ggctccctctCTTCcgtctcttc-3′.

Luciferase Assay

The pXP-214 kb/-0.334 kb/Luc plasmid containing the 3.5kb −15/−14 URE cloned 5′ of the PU.1 minimal promoter was cloned upstream of the Luciferase reporter [17]. A construct containing a 1.5kb segment 5′ of *SCL* promoter *1a* in addition to promoter *1a* and *1b* was cloned upstream of Luciferase reporter gene in the pGL2 vector [18](SCL-pGL2 plasmid). Control and *ZBP89*-silenced MEL cells were transiently transfected with SCL-pGL2 or pXP-214 kb/-0.334 kb/Luc plasmids. QM7 cells intrinsically lacking ZBP-89 were co-transfected with luciferase reporter constructs prepared using the wild-type G1HE-(124-235)-luc) or G4 mutant G1HE-(124-235)-Luc reporter [12] and an expression plasmid

encoding wild type mouse ZBP-89. Transfected cells were harvested, washed twice in PBS, pelleted, lysed with 300μl of lysis buffer (Promega Inc., WI) for 30 minutes at room temperature, and lysate centrifuged for 10 minutes at 13,000 rpm. Luciferase assays were carried out on 20μl of each cell lysate supernatant and light units measured in a Berthold LB9507 luminometer (Berthod, Germany). Relative light units were normalized for transfection efficiency against β-Gal values obtained from 20μl of each supernatant. β-Galactosidase (β-Gal) assays were performed according to the manufacturer's instructions (Applied Biosystems).

Statistical Analysis

The significance of the difference between groups in the *in vitro* and *in vivo* experiments was determined by analysis of variance followed by a one-tailed Student's t test. Data are expressed as the mean±SD, with P-values of < 0.05 considered significant.

Results

Anemia and thrombocytopenia in *ZBP-89* CKO mice

We conditionally inactivated *ZBP-89* in the mouse hematopoietic system by breeding a *ZBP-89*$^{fl/fl}$ C57BL/6 mouse strain [11] with interferon-inducible *Mx-Cre* transgenic C57BL/6 mice [19](Fig. 1A), followed by administration of poly(I)-poly(C) (pIpC) every other day for a total of 7 injections. PCR of genomic DNA from control (*ZBP-89*$^{fl/fl}$-*Mx*$^{Cre-}$) and *ZBP-89*$^{fl/fl}$-*Mx*$^{Cre+}$ mice showed undetectable amounts of *ZBP-89*$^{fl/fl}$ in single BM-derived colony forming-unit-Granulocyte-Macrophage (CFU-GM) colonies transduced with the *Cre* gene, indicating nearly complete excision of both *ZBP-89*$^{fl/fl}$ alleles (Fig. 1B).

PB cells obtained weekly in the first 4 weeks and at 2 months after the last pIpC injection showed a significant drop in red blood cells (RBC) and hemoglobin (Hgb) and in platelet counts and in CD41^{+} megakaryocytes in *ZBP-89*$^{-/-}$-*Mx*$^{Cre+}$ mice but not in control (*ZBP-89*$^{fl/fl}$-*Mx*^{Cre}) mice 3 weeks after the last pIpC injection (Fig. 1C, 1D). No significant changes in peripheral white blood count (WBC), or circulating myeloid (CD11b^{+}), lymphoid T- (CD3^{+}) or B- (B220^{+}) cells were detected (Fig. 1C, D). Consistently, bone marrow colony forming assays showed reduced *ZBP-89*-deficient burst-forming unit-erythroid (BFU-E) and Granulocyte-Erythroid-Macrophage-Megakaryocyte (GEMM), but not CFU-GM, CFU-M or CFU-G colonies (Supplemental Figure 2A). Peripheral RBC and platelet counts returned to normal at 4 and 8 weeks post pIpC (Fig. 1C), with an associated normalization of bone marrow BFU-E and CFU-GEMM colony counts of *ZBP-89*CKO mice (Supplemental Figure 2B).

Changes in HSPC and their transcriptional profile

The percentage of *ZBP-89*-deficient MEP was significantly reduced 3 weeks post pIpC (Fig. 2A), but no change was detected in *ZBP-89*-deficient LT-HSC, MPP, CMP, CLP, GMP and MEP.

The transcriptional profiles of key transcription factors known to regulate hematopoietic lineage commitment were measured in BM progenitors from *ZBP-89*-deficient and sufficient animals (Fig. 2B). RT-PCR carried out on mRNA derived from sorted *ZBP-89*-deficient MPP, CLP, CMP, GMP and MEP revealed a significant induction of *PU.1* in MPP, CLP, CMP and MEP, and of *FOXO1* in *ZBP-89*-deficient MPP and CLP. In contrast, *SCL/TAL1* and *GATA1* levels were significantly reduced by ~60–80% in *ZBP-89*-deficient MPP, CMP and MEP but not in CLP or GMP. *TIF1γ* was only suppressed in MEP, while *C/EBPα* was suppressed in MPP, CMP and GMP (Fig. 2B). As expected, *ZBP-89* mRNA levels were minimal in HSPC derived from *ZBP-89* CKO mice (Fig. 2B).

ZBP-89 contributes to the erythro- and megakaryopoietic reserve in the adult

In response to erythroid stress in adults, the rate of RBC production rapidly increases from its steady state level [20]. We evaluated the response to acute depletion of RBC or platelets in *ZBP-89* CKO and control mice. Phenylhydrazine (PHZ) induced a significant (~50%) drop in circulating RBC counts (Fig. 3A) and in bone marrow BFU-E colonies (Supplemental Figure 2C), but not in peripheral blood platelet counts (Fig. 3A) or CFU-GEMM colonies (Supplemental Figure 2C) from *ZBP-89* CKO mice. Erythroblast development was examined using two methods [14, 15], both of which showed a significant reduction in pro- and basophilic erythroblasts of *ZBP-89* CKO mice (Fig. 3B, Supplemental Figure 3), in parallel with an increase in pro- and basophilic erythroblasts in spleen of *ZBP-89* CKO mice (Fig. 3B, Supplemental Figure 3A, B). Polychromatic erythroblasts in spleen were increased ~1.6-fold in *ZBP-89* CKO mice when quantified by one method [14] (Fig. 3B) but not the other [15] (Supplemental Figure 3B). There was also a significant increase in spleen size on day 5 after PHZ injection in *ZBP-89* CKO mice (Supplemental Figure 4). These changes were insufficient, however, to prevent stress-induced anemia on day 5, but might have contributed to the normalization of RBC, Hb and Hct by day 15 after PHZ injection (Supplemental Figure 5).

PB platelet count, but not RBC or WBC counts, also significantly decreased in *ZBP-89* CKO mice upon acute administration of 5-fluorouracil (5-FU), which depletes immature megakaryocytic progenitors and megakaryocytes in endomitosis [21](Fig. 3C). FACS analysis further confirmed that the megakaryocyte lineage marker CD41 was markedly reduced in PB following 5-FU treatment (Fig. 3D), with no significant changes in PB myeloid ($CD11b^+$), T- ($CD3^+$), or B-cells ($B220^+$).

ZBP-89 deletion results in reciprocal changes in the myeloid- and B-cell lineages in BM repopulation assays

$CD45.2^+$ BM cells from *ZBP-89*-excised (*ZBP-8*$^{-fl/fl}$-*Mx*$^{Cre+}$) and control (*ZBP-89*$^{fl/fl}$-*Mx*$^{Cre-}$) mice were transplanted into congenic lethally irradiated $CD45.1^+$ recipients that were then treated with pIpC starting 6 weeks after transplantation (Fig. 4 A). The contribution of *ZBP-89*-excised $CD45.2^+$ hematopoietic stem cells to PB and BM cells was monitored by surface expression of the CD45.2 allele in HSPC and in PB (Fig. 4 B–E). The proportion of $CD45.1^+$ and of $CD45.2^+$ cells in recipients 3 weeks after primary BMT was equivalent (Fig. 4B, upper panel). Since partially differentiated, yet multi-lineage hematopoietic precursors continue to generate mature cells for up to 3 months post BMT, we measured the percentage of progenitors and differentiated blood cells that descended from donor and competitor precursors up to 8 months after BMT, thus ensuring that all mature blood cells derive from primitive hematopoietic stem cells [22, 23]. *ZBP-89*-excised $CD45.2^+$ cells contributed comparably to peripheral myeloid and lymphoid cells ($CD11b^+$, $CD3^+$ and $B220^+$) in recipient mice for 4.5 months (Fig. 4C). Afterwards, the $CD45.2^+$ $CD11b^+$ PB pool dropped significantly (by ~2/3rd) with a reciprocal increase in the $B220^+$ pool, but with no changes in number of $CD3^+$ cells. At 3 weeks post pIpC, $CD45.2^+$ $CD41^+$ megakaryocytic cell numbers signficantly dropped, but normalized at week 6 post pIpC onwards (Fig. 4C), as in the steady state (Fig. 1C). RBC levels were normal but their origin was not determined in the chimeric mice as RBC lack CD45 expression. A significant reduction in GMP with a corresponding increase in Pre-B and a drop in Pre-Pro-B were observed in the BM, 38 weeks post pIpC (Fig. 4D, E). These changes likely account for the reciprocal alterations in *ZBP-89*-excised $CD45.2^+$ $CD11b^+$ and $CD45.2^+$ $BB20^+$ cells in peripheral blood. No changes were detected in the LT-HSC, CMP, MEP or Pro-B pools (Fig. 4 D, E). The decrease in the Pre-Pro-B cells and the increase in the Pre-B population (Fig. 4E) may suggest that proliferation of *ZBP-89*-excised B-cell progenitors in the stages from Pro-B to Pre-B cells is accelerated.

We next examined the capacity of *ZBP-89*-excised CD45.2$^+$ BM HSC for long-term reconstitution of adult hematopoiesis by serial transplantation. Donor CD45.2$^+$ *ZBP-89*$^{-/-}$ or *ZBP-89*$^{fl/fl}$ BM (as control) cells were injected into lethally irradiated CD45.1$^+$ recipient mice. The multi-lineage engraftment potential was assessed over an 8-month period. A reduction in PB CD11b$^+$CD45.2$^+$ cells and an increase in B220$^+$CD45.2$^+$ cells were again seen in cells derived from *ZBP-89*-excised HSPC, beginning earlier (at week 6-post transplantation) (Fig. 5A) vs. 24 weeks following primary BMT (Fig. 4C). Examination of BM hematopoietic progenitors at 7.5 months also showed persistence in the contraction of the GMP pool size and the increase in the Pre-B compartment (Fig. 5 B, C).

Transcriptional deregulation in *ZBP-89*-excised HSPC

RT-PCR analysis performed on RNA derived from sorted *ZBP-89*-deficient BM **HSPC** from secondary BM transplant recipient mice at 36 weeks post transplantation showed persistent upregulation of *PU.1* and downregulation of *GATA1* and *SCL/TAL1* in MPP, CMP and MEP, upregulation of *FOXO1* in MPP and downregulation of *C/EBPα* in MPP, CMP and GMP, and of *Gif1* in MPP and *FOG-1* in MEP (Fig. 5D). No significant changes in *C-myb* or *Tif-1γ* expression were seen.

The hematopoietic lineage anomalies in ZBP-89 CKO mice are reproduced *in vitro* in *ZBP-89*-silenced multipotent A4 cells

As previously described [24], immunophenotyping of wild-type A4 cells by flow cytometry showed that the bulk express the B lineage marker B220, the myeloid lineage marker CD11b and the megakaryocytic marker CD41 (Table 1). Stable silencing of ZBP-89 in A4 progenitors caused significant reductions in expression of CD41 and CD1b but increased expression of B220, mirroring the changes observed under BMT stress conditions *in vivo*. RT-PCR analysis performed on RNA derived from *ZBP-89*-sufficient and deficient A4 progenitors again showed downregulation of *GATA1*, *SCL/TAL1* and *C/EBPα* and upregulation of *PU.1* and *FOXO1* in *ZBP-89*-silenced cells (Fig. 5E).

ZBP-89 acts as a direct transcriptional repressor of *PU.1* and activator of *SCL* and *GATA1*

Induction of *PU.1*, and suppression of *SCL* in *ZBP-89*-silenced BM progenitors, suggested these two factors might be direct downstream targets of ZBP-89, as has been previously shown for *GATA1*[12]. This was tested (Fig. 6A–F) using ChIP [16] and luciferase reporter assays in WT and *ZBP-89*-silenced MEL cells or in the non-hematopoietic QM7 cells, which lack endogenous ZBP-89 [12], using the known transcriptional regulation of GATA1 by ZBP-89 as a positive control (Fig. 6A–C).

Expression of PU.1 is regulated primarily by a −15/14 kb upstream regulatory region (URE) (Fig. 6D), deletion of which reduces PU.1 expression by 80% in mice [25]. C/EBPα binds to URE and prepares an adjacent −12kb enhancer for autoregulatory PU.1 chromatin entry, thus driving myeloid-specific PU.1 expression [26]. A Genomatix search [27] identified 3 potential ZBP-89 binding sites in the −15/14 kb URE (Fig. 6E), two of which overlap. ChIP assays confirmed binding of ZBP-89 to URE (Fig. 6D, lower panel). Luciferase reporter assays carried out on WT and *ZBP-89*-silenced MEL transiently transfected with the pXP-214 kb/-0.5 kb/Luc plasmid [25] (Fig. 6E), revealed a ~2.5 fold induction of PU.1 when ZBP-89 was silenced (Fig. 6F).

Tissue-specific expression of murine (and human) *SCL* is driven by 2 minimal promoters *1a* and *1b* [28] (Fig. 6G). Promoter *Ia* restricts *SCL* expression to the erythroid lineage [18], and *Ib* directs *SCL* expression in CD34$^+$ hematopoietic progenitors [29]. A Genomatix search revealed two potential ZBP-89 binding sites in the immediate 5′ regions of *1a* and *1b* in *SCL* (Fig. 6H). ChIP assays in WT MEL cells showed that ZBP-89 binds specifically to DNA

fragments containing these regions upstream of the respective promoter (Fig. 6G, lower panel). Luciferase reporter assays showed that the *-2kbSCL1a1b* region drove luciferase expression in WT MEL cells, but minimally in *ZBP-89*-silenced MEL (the residual activity is likely explained by the incomplete 80% silencing of ZBP-89). Nucleotide substitutions of one or both consensus ZBP-89 binding motifs reduced luciferase reporter activity by 50% and by 60%, respectively (Fig. 6I), suggesting that ZBP-89 binding to the proximal site plays a greater role in *SCL* induction in the WT MEL cellular context.

Discussion

The role of ZBP-89 in embryonic development of the hematopoietic system has been previously described in zebrafish and mouse embryos [8, 9]. Using a conditional knockout model of ZBP-89 in adult mice, we now show that ZBP-89 plays a previously unrecognized role in stress hematopoiesis in the adult.

Excision of ZBP-89 in adult mice resulted in the overt drop in circulating RBC and platelet counts by 3 weeks post pIpC but spared the other hematopoietic lineages, despite the efficient excision of *ZBP-89* in the respective hematopoietic progenitors. Anemia and thrombocytopenia were associated with a significant reduction in MEP and in early and late erythroid progenitors in bone marrow, findings that were also observed in the absence of the master erythroid megakaryocytic regulator GATA1 [30]. This is likely secondary to the higher myeloid potential of CMP and MPP, resulting from reduced GATA1 and increased PU.1 expression in these progenitors [1, 6, 31, 32].

The anemia and thrombocytopenia observed in *ZBP-89* CKO mice were however transient, with normalization of RBC and platelet counts in PB 4 and 8 weeks post pIpC, in parallel with normalization of BFU-E and CFU-GEMM BM colonies at 8 weeks post pIpC. This recovery is unlikely to derive from progenitors that escaped *Cre*-excision of the *ZBP-89* gene, since *ZBP-89* excision in hematopoietic progenitors is still demonstrable 36 months later (Fig. 5D). A more likely explanation is that loss of ZBP-89 in BM progenitors can be overcome *in vivo* in the steady state. The redundancy sometimes observed in genetic ablation models is usually explained by the presence of a functionally related gene. Whether ZBP-99 (ZNF281), the other known member of the ZBP-89 family [33], can compensate for loss of ZBP-89 in early BM erythro-megakaryocytic progenitors in the steady state will require further study.

The defect in the erythro-megakaryocytic lineages in *ZBP-89* CKO mice can readily be exposed under stress (Fig. 3). Hemolytic stress normally induces expansion of erythroid progenitors in the spleen, driven largely by rapid proliferation of erythroid progenitors [34]. The response to stress erythropoiesis in mice, which occurs mainly in the spleen [35], was evident in *ZBP-89* CKO mice, but insufficient to prevent overt anemia. Erythropoiesis in the spleen is a molecularly distinct process from BM erythropoiesis, dependent on the glucocorticoid receptor [36], c-Kit [35] and BMP4/Smad5 [37], which may explain the differential response to stress in the spleen vs. that in BM of *ZBP-89* CKO mice. Impaired development and maturation of the erythroid lineage in BM under stress in *ZBP-89* CKO mice has also been observed in *GATA1* CKO mice [30] and to a lesser degree in *SCL/TAL1* CKO mice [38], suggesting that abnormal stress erythropoiesis in *ZBP-89* deficient BM erythroid progenitors is likely caused by suppressed expression of one or both of these factors.

Ablation of ZBP-89 in hematopoietic cells following competitive transplantation of whole BM from CD45.2$^+$ *ZBP-89*$^{fl/fl}$-*Mx*$^{Cre+}$ *or ZBP-89*$^{fl/fl}$-*Mx*$^{Cre-}$ (control) mice and pIpC treatment again lead to the early drop in circulating CD41$^+$ cells at 3 weeks post pIpC, similar to that observed in non transplanted *ZBP-89* CKO mice in the steady state. Follow

up of primary BMT recipient mice, however, revealed a significant and persistent drop in circulating $CD11b^+$ cells and an increase in $B220^+$ cells by 24 weeks post transplant (Fig. 4C), together with a significant decrease in GMP and an increase in Pre-B BM progenitors (Fig. 4D, E). The reciprocal changes in the progenitor cell pools were also seen earlier (by 6 weeks) following secondary transplantation, which persisted for at least 30 weeks (Fig. 5A). The above lineage anomalies were reproduced *in vitro* by stable knock down of *ZBP-89* in the multipotent A4 cells (Table 1), suggesting that the changes in the hematopoietic progenitors observed in whole animals are cell-autonomous, and directly related to loss of ZBP-89.

Selective transcriptional profiling showed increased *PU.1* and suppressed *GATA1* and *SCL* expression in MPP, CMP and MEP from *ZBP-89* CKO mice (Fig. 2B and 5D) and in *ZBP-89*-silenced A4 cells (Fig. 5E). These changes are expected to favor development of the myeloid lineage, based on the binary model of HSC fate decisions. Yet, the measured outcome was a reduction in the myeloid lineage, with a reciprocal increase in the B lymphoid lineage. One potential explanation is the observed concomitant reduction of C/EBPα in *ZBP-89*-deficient myeloid progenitors (Fig. 5D), which is also observed in *ZBP-89*-silenced A4 cells (Fig. 5E). The reduction of C/EBPα in GMP compartment could compromise the ability of PU.1 to access the autoregulatory −12kb enhancer element in this pool, which is necessary for its commitment to the myelomonocytic cell lineage [5, 26]. This myeloid lineage defect, which is not seen under steady state conditions, is readily uncovered under the replicative stress imposed by serial BMT, which could lead to exhaustion of the GMP pool [39]. Formation of a complex of PU.1/E2A/FOXO1 on the −14kb URE in *ZBP-89*-deficient CLP, where *PU.1* is also upregulated, appears sufficient, however, for growth and differentiation of the B cell lineage [26, 40, 41], enhanced in this case by the concomitant upregulation of *FOXO1* in this population.

CHIP and luciferase reporter assays show that ZBP-89 acts directly to repress PU.1 while activating both SCL and GATA1, consistent with the lineage anomalies induced *in vitro* by loss of ZBP-89 in A4 cells. The reciprocal regulation of C/EBPα and FOXO1 by ZBP-89 in hematopoietic progenitors that is seen both *in vivo* (Fig. 2B, 5D), and *in vitro* (Fig. 5E) may also be direct (both promoters have potential ZBP-89 binding motifs) or indirect, driven by modulated expression of one or more of the other regulated genes.

In conclusion, we have provided evidence that ZBP-89 plays an important role in stress hematopoiesis in adult mice. Identification of ZBP-89 as an important modulator of key lineage-determining genes provides new insights into the genetic programs that underlie lineage decisions in adult hematopoiesis under steady state and stress conditions.

Supplementary Material

Refer to Web version on PubMed Central for supplementary material.

Acknowledgments

We thank Dr. Hanno Hock (MGH Cancer Center) for providing *MX1-Cre* transgenic mice, Dr. Daniel Tenen (BIDMC, Boston, MA) and Dr. Kinuko Ohneda (Takasaki University of Health and Welfare, Takasaki, Japan) for plasmids and Dr. Ursula Just (University of Kiel, Germany) for FDCP-Mix A4 cells. This work was supported by NIH grants DK081920 (to MAA) and DK55732 (to JLM) from the National Institutes of Health (NIDDK).

References

1. Iwasaki H, Mizuno S, Wells RA, et al. GATA-1 converts lymphoid and myelomonocytic progenitors into the megakaryocyte/erythrocyte lineages. Immunity. 2003; 19:451–462. [PubMed: 14499119]
2. Rosenbauer F, Tenen DG. Transcription factors in myeloid development: balancing differentiation with transformation. Nature reviews Immunology. 2007; 7:105–117.
3. Fujiwara T, O'Geen H, Keles S, et al. Discovering hematopoietic mechanisms through genome-wide analysis of GATA factor chromatin occupancy. Molecular cell. 2009; 36:667–681. [PubMed: 19941826]
4. Yu M, Riva L, Xie H, et al. Insights into GATA-1-mediated gene activation versus repression via genome-wide chromatin occupancy analysis. Molecular cell. 2009; 36:682–695. [PubMed: 19941827]
5. Yeamans C, Wang D, Paz-Priel I, et al. C/EBPalpha binds and activates the PU.1 distal enhancer to induce monocyte lineage commitment. Blood. 2007; 110:3136–3142. [PubMed: 17671233]
6. Arinobu Y, Mizuno S, Chong Y, et al. Reciprocal activation of GATA-1 and PU.1 marks initial specification of hematopoietic stem cells into myeloerythroid and myelolymphoid lineages. Cell stem cell. 2007; 1:416–427. [PubMed: 18371378]
7. Merchant JL, Iyer GR, Taylor BR, et al. ZBP-89, a Kruppel-like zinc finger protein, inhibits epidermal growth factor induction of the gastrin promoter. Molecular and cellular biology. 1996; 16:6644–6653. [PubMed: 8943318]
8. Li X, Xiong JW, Shelley CS, et al. The transcription factor ZBP-89 controls generation of the hematopoietic lineage in zebrafish and mouse embryonic stem cells. Development. 2006; 133:3641–3650. [PubMed: 16914492]
9. Woo AJ, Moran TB, Schindler YL, et al. Identification of ZBP-89 as a novel GATA-1-associated transcription factor involved in megakaryocytic and erythroid development. Molecular and cellular biology. 2008; 28:2675–2689. [PubMed: 18250154]
10. Just U, Stocking C, Spooncer E, et al. Expression of the GM-CSF gene after retroviral transfer in hematopoietic stem cell lines induces synchronous granulocyte-macrophage differentiation. Cell. 1991; 64:1163–1173. [PubMed: 2004422]
11. Essien BE, Grasberger H, Romain RD, et al. ZBP-89 Regulates Expression of Tryptophan Hydroxylase I and Mucosal Defense Against Salmonella Typhimurium in Mice. Gastroenterology. 2013; 144:1466–1477. e1469. [PubMed: 23395646]
12. Ohneda K, Ohmori S, Ishijima Y, et al. Characterization of a functional ZBP-89 binding site that mediates Gata1 gene expression during hematopoietic development. The Journal of biological chemistry. 2009; 284:30187–30199. [PubMed: 19723625]
13. Gurumurthy S, Xie SZ, Alagesan B, et al. The Lkb1 metabolic sensor maintains haematopoietic stem cell survival. Nature. 2010; 468:659–663. [PubMed: 21124451]
14. Socolovsky M, Nam H, Fleming MD, et al. Ineffective erythropoiesis in Stat5a(−/−) 5b(−/−) mice due to decreased survival of early erythroblasts. Blood. 2001; 98:3261–3273. [PubMed: 11719363]
15. Liu J, Zhang J, Ginzburg Y, et al. Quantitative analysis of murine terminal erythroid differentiation in vivo: novel method to study normal and disordered erythropoiesis. Blood. 2013; 121:e43–49. [PubMed: 23287863]
16. Gutierrez S, Liu J, Javed A, et al. The vitamin D response element in the distal osteocalcin promoter contributes to chromatin organization of the proximal regulatory domain. The Journal of biological chemistry. 2004; 279:43581–43588. [PubMed: 15299011]
17. Okuno Y, Huang G, Rosenbauer F, et al. Potential autoregulation of transcription factor PU.1 by an upstream regulatory element. Molecular and cellular biology. 2005; 25:2832–2845. [PubMed: 15767686]
18. Bockamp EO, McLaughlin F, Murrell AM, et al. Lineage-restricted regulation of the murine SCL/TAL-1 promoter. Blood. 1995; 86:1502–1514. [PubMed: 7632958]
19. Kuhn R, Schwenk F, Aguet M, et al. Inducible gene targeting in mice. Science. 1995; 269:1427–1429. [PubMed: 7660125]

20. Peschle C, Magli MC, Cillo C, et al. Kinetics of erythroid and myeloid stem cells in post-hypoxia polycythaemia. British journal of haematology. 1977; 37:345–352. [PubMed: 603766]
21. Chenaille PJ, Steward SA, Ashmun RA, et al. Prolonged thrombocytosis in mice after 5-fluorouracil results from failure to down-regulate megakaryocyte concentration. An experimental model that dissociates regulation of megakaryocyte size and DNA content from megakaryocyte concentration. Blood. 1990; 76:508–515. [PubMed: 2378983]
22. Jordan CT, Lemischka IR. Clonal and systemic analysis of long-term hematopoiesis in the mouse. Genes & development. 1990; 4:220–232. [PubMed: 1970972]
23. Morrison SJ, Weissman IL. The long-term repopulating subset of hematopoietic stem cells is deterministic and isolatable by phenotype. Immunity. 1994; 1:661–673. [PubMed: 7541305]
24. Ford AM, Healy LE, Bennett CA, et al. Multilineage phenotypes of interleukin-3-dependent progenitor cells. Blood. 1992; 79:1962–1971. [PubMed: 1373332]
25. Iwasaki H, Somoza C, Shigematsu H, et al. Distinctive and indispensable roles of PU.1 in maintenance of hematopoietic stem cells and their differentiation. Blood. 2005; 106:1590–1600. [PubMed: 15914556]
26. Leddin M, Perrod C, Hoogenkamp M, et al. Two distinct auto-regulatory loops operate at the PU.1 locus in B cells and myeloid cells. Blood. 2011; 117:2827–2838. [PubMed: 21239694]
27. Cartharius K, Frech K, Grote K, et al. MatInspector and beyond: promoter analysis based on transcription factor binding sites. Bioinformatics. 2005; 21:2933–2942. [PubMed: 15860560]
28. Begley CG. The SCL transcription factor and differential regulation of macrophage differentiation by LIF, OSM and IL-6. Stem Cells. 1994; 12 (Suppl 1):143–149. discussion 149–151. [PubMed: 7696958]
29. Bockamp EO, Fordham JL, Gottgens B, et al. Transcriptional regulation of the stem cell leukemia gene by PU.1 and Elf-1. The Journal of biological chemistry. 1998; 273:29032–29042. [PubMed: 9786909]
30. Gutierrez L, Tsukamoto S, Suzuki M, et al. Ablation of Gata1 in adult mice results in aplastic crisis, revealing its essential role in steady-state and stress erythropoiesis. Blood. 2008; 111:4375–4385. [PubMed: 18258797]
31. Walsh JC, DeKoter RP, Lee HJ, et al. Cooperative and antagonistic interplay between PU.1 and GATA-2 in the specification of myeloid cell fates. Immunity. 2002; 17:665–676. [PubMed: 12433372]
32. Nerlov C, Graf T. PU.1 induces myeloid lineage commitment in multipotent hematopoietic progenitors. Genes & development. 1998; 12:2403–2412. [PubMed: 9694804]
33. Law DJ, Du M, Law GL, et al. ZBP-99 defines a conserved family of transcription factors and regulates ornithine decarboxylase gene expression. Biochemical and biophysical research communications. 1999; 262:113–120. [PubMed: 10448078]
34. Mide SM, Huygens P, Bozzini CE, et al. Effects of human recombinant erythropoietin on differentiation and distribution of erythroid progenitor cells on murine medullary and splenic erythropoiesis during hypoxia and post-hypoxia. In Vivo. 2001; 15:125–132. [PubMed: 11317516]
35. Broudy VC, Lin NL, Priestley GV, et al. Interaction of stem cell factor and its receptor c-kit mediates lodgment and acute expansion of hematopoietic cells in the murine spleen. Blood. 1996; 88:75–81. [PubMed: 8704204]
36. Bauer A, Tronche F, Wessely O, et al. The glucocorticoid receptor is required for stress erythropoiesis. Genes & development. 1999; 13:2996–3002. [PubMed: 10580006]
37. Lenox LE, Perry JM, Paulson RF. BMP4 and Madh5 regulate the erythroid response to acute anemia. Blood. 2005; 105:2741–2748. [PubMed: 15591122]
38. Hall MA, Slater NJ, Begley CG, et al. Functional but abnormal adult erythropoiesis in the absence of the stem cell leukemia gene. Molecular and cellular biology. 2005; 25:6355–6362. [PubMed: 16024775]
39. Harrison DE, Astle CM, Delaittre JA. Loss of proliferative capacity in immunohemopoietic stem cells caused by serial transplantation rather than aging. The Journal of experimental medicine. 1978; 147:1526–1531. [PubMed: 25943]
40. DeKoter RP, Singh H. Regulation of B lymphocyte and macrophage development by graded expression of PU.1. Science. 2000; 288:1439–1441. [PubMed: 10827957]

41. Xie H, Ye M, Feng R, et al. Stepwise reprogramming of B cells into macrophages. Cell. 2004; 117:663–676. [PubMed: 15163413]

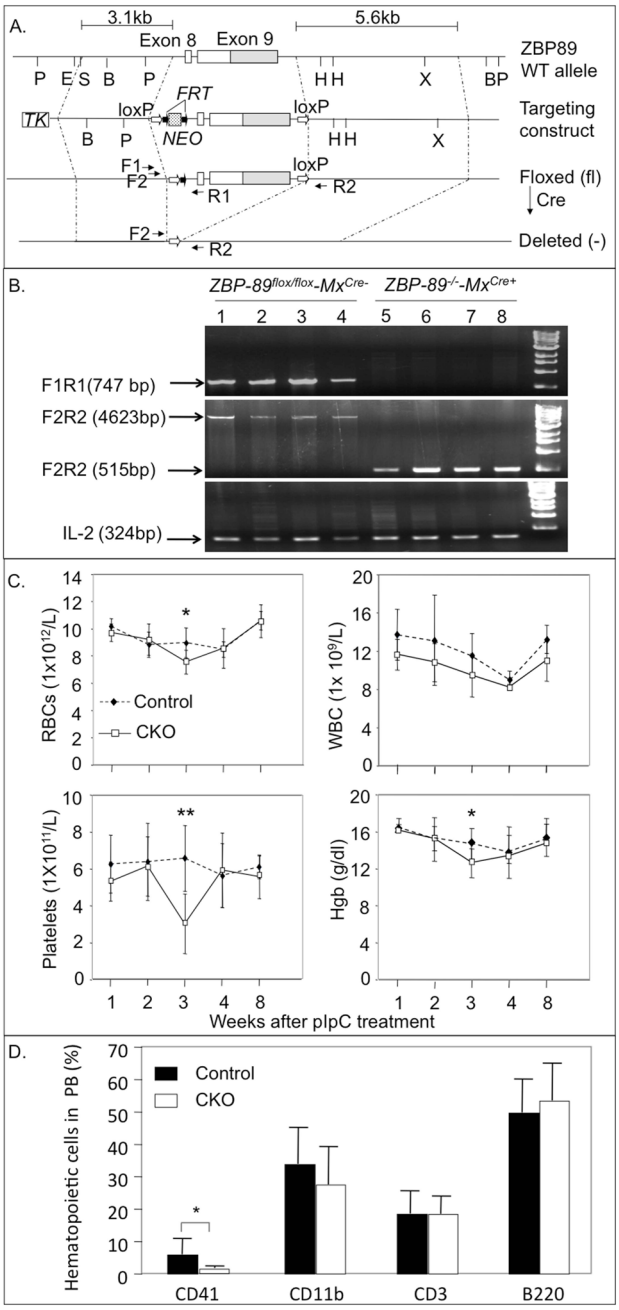

Figure 1. Generation and PB phenotype of *ZBP-89* CKO mice

(A) Strategy for inducible inactivation of *ZBP89* in HSPC. Schematic of targeted *ZBP-89* exons 8 and 9 (in white), with non-coding region of exon 9 in gray. Restriction sites (P, PstI; E, EcoR1; B, BamH1; H, HindIII; X, Xba1), LoxP sites (open arrows) and FRT sites (closed arrows) are indicated. F1, F2, R1 and R2 represent approximate position and orientation of the primers used in PCR. *TK*, thymidine kinase; *NEO*, neomycin. Sizes of the left (3.1kb) and right (5.6kb) vector arms are shown. (B) PCR genotyping showing deletion of the floxed segment of *ZBP-89* in single CFU-GM stem cell colonies 8 weeks after pIpC treatment. Lanes 1–4, BM colonies from control (*ZBP-89*$^{fl/fl}$-*Mx*$^{Cre-}$) mice, and lanes 5–8 are colonies from *ZBP-89* CKO (*ZBP-89*$^{-/-}$-*Mx*$^{Cre+}$) mice post pIpC. IL2 is included as

internal control. (C) PB white blood cells (WBC)-, RBC-, and platelet counts and hemoglobin (Hgb) level 1–8 weeks after pIpC in (C) PB white blood cells (WBC)-, RBC-, and platelet counts and hemoglobin (Hgb) level 1–8 weeks after pIpC in six control mice (filled diamonds, dotted lines) and in seven *ZBP-89* CKO mice (open squares, solid lines). Results are shown as mean ± SD, from 2 independent experiments. *P < 0.05, **P < 0.01. (D) $CD41^+$, $CD11b^+$, $CD3^+$ and $B220^+$ cells in PB from normal (open bars) and *ZBP89* CKO mice (black bars) 3 weeks after pIpC injections (mean ± SD, n=6 in each group).

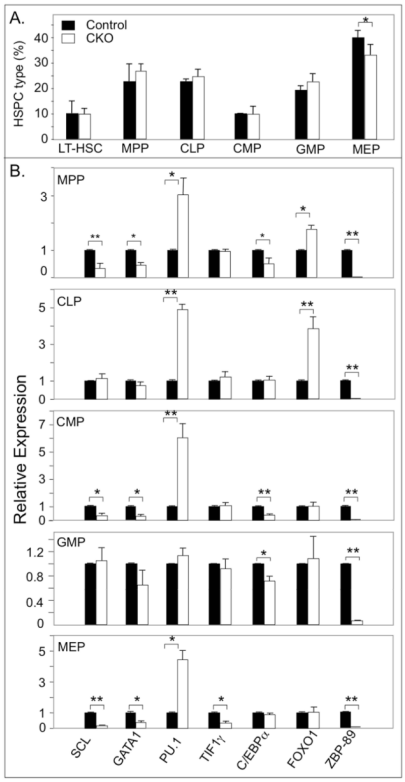

Figure 2. Transcription factor profiles of BM HSPC from *ZBP-89* CKO and control mice 3 weeks after the last dose of pIpC

(A) Histograms (mean ± SD, n=3) showing the percentage of LT-HSC and MPP, CLP, CMP, GMP and MEP in fractionated BM cells from *ZBP-89* CKO and in control mice. (B) RT-PCR analysis of transcription factors in BM progenitors derived from *ZBP-89* CKO and control mice (bars are colored as in A). Results are from two independent experiments, each representing pooled samples from two mice in each group. * P<0.05; ** P<0.01.

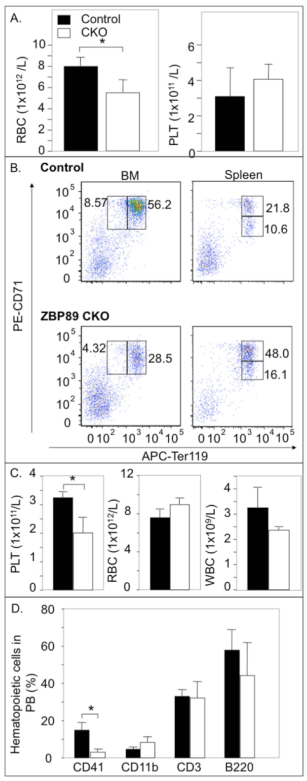

Figure 3. Effect of *ZBP-89* CKO on stress erythropoiesis and thrombopoiesis

(A) Histograms (mean ± SD, n=4) showing the effect of PHZ-induced hemolysis on RBC and platelet (PLT) counts in PB of *ZBP-89* CKO mice (white bars here and in C, D) compared to control mice (black bars here and in C, D). (B) Representative FACS analyses of BM proerythroblasts ($CD71^{high}Ter119^{low}$) and basophilic erythroblasts ($CD71^{high}Ter119^{high}$) (left) and in basophilic- and in polychromatic ($CD71^{low}Ter119^{high}$) erythroblasts in spleen (right) of control and *ZBP-89* CKO mice, two weeks after the last pIpC injection and 5 days after PHZ. Numbers for each box reflect percentages of the gated cells, with each representing the mean value from four mice in each group. (C, D) Histograms (mean ± SD, n=4) showing the effect of 5-fluorouracil (5-FU)-induced platelet depletion on circulating platelet-, white blood cells (WBC)- and RBC counts (C), and on surface phenotype, analyzed by FACS from *ZBP-89* CKO and control mice, two weeks after the last pIpC treatment and 6 days after 5-FU (D). * $P<0.05$.

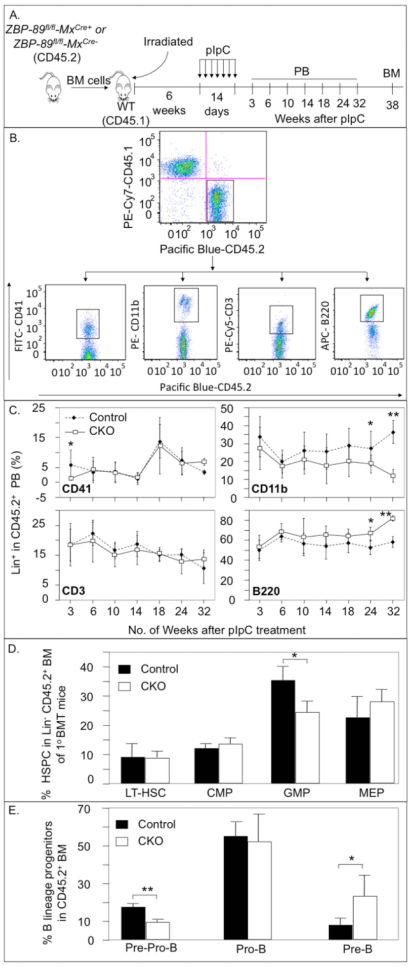

Figure 4.

PB cell counts and percentage of immature hematopoietic lineages in 1° BM transplant recipients. (A) Schematic of the experimental design: BM cells (CD45.2$^+$) from *ZBP-89* CKO and control mice were mixed with wild type (WT, CD45.1$^+$) BM cells at a 1:1 ratio and the mixture injected into irradiated wild-type (WT) recipients (CD45.1$^+$). pIpC injections started 6 weeks later and over a 2-week period. PB samples were analyzed at 3–32 weeks after the last pIpC dose and BM was examined at 38 weeks. (B) Isolation of lineage-specific CD45.2$^+$CD45.1$^-$ PB cells from control recipients of 1° BM at 3 weeks post pIpC. (C) Percentage of PB megakaryocytes (CD41$^+$), myeloid- (CD11b$^+$), T- (CD3$^+$) and B (B220$^+$)-cells in the CD45.2$^+$ population of *ZBP-89*$^{-/-}$ and control (*ZBP-89*$^{fl/fl}$) mice at the indicated times after pIpC injections. (D) Histograms showing percentage of the different immature hematopoietic lineages in the CD45.2$^+$ BM population of *ZBP-89*$^{-/-}$ (mean ± SD, n=7) and control mice (mean ± SD, n=8) 38 weeks after pIpC treatment. (E) Histograms (mean ± SD, n=4) showing the percentage of Pre-Pro-B cells, Pro-B cells and Pre-B cells in the CD45.2$^+$ BM population of *ZBP-89*$^{-/-}$ and control mice 38 weeks after pIpC treatment. * P<0.05, **P<0.01.

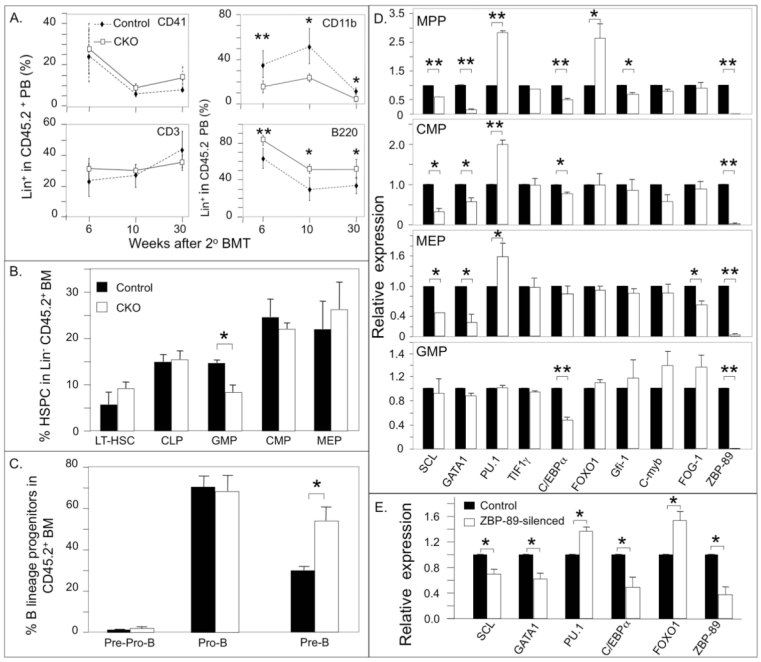

Figure 5. Hematopoietic lineages and their transcriptional profiles in 2° BM transplant recipients and in *ZBP-89*-silenced A4 cells

(A) Percentages of the different HSPC lineages in CD45.2$^+$ PB at different times after 2° BM transplantation. Results given are mean ± SD (n=5 mice in each group). (B, C) Histograms (mean ± SD, n=4) showing the percentages of the different BM progenitors in CD45.2$^+$ BM from 2nd BMT recipients at 30 weeks post transplantation from control (black bars) and CKO mice (white bars). * P<0.05, ** P<0.01. (D) Histograms (mean ± SD, n=2 independent experiments) showing gene expression profiles in BM progenitors from *ZBP-89*-deficient cells 36 weeks after 2° BMT (white bars) relative to that in control mice (black bars). For each experiment, RNAs from two mice in each group were pooled for RT-PCR. * P<0.05; ** P<0.01. (E) Histograms (mean ± SD, n=2 experiments) showing gene expression profiles in control and Z*BP-89*-silenced A4 progenitors. * P<0.05.

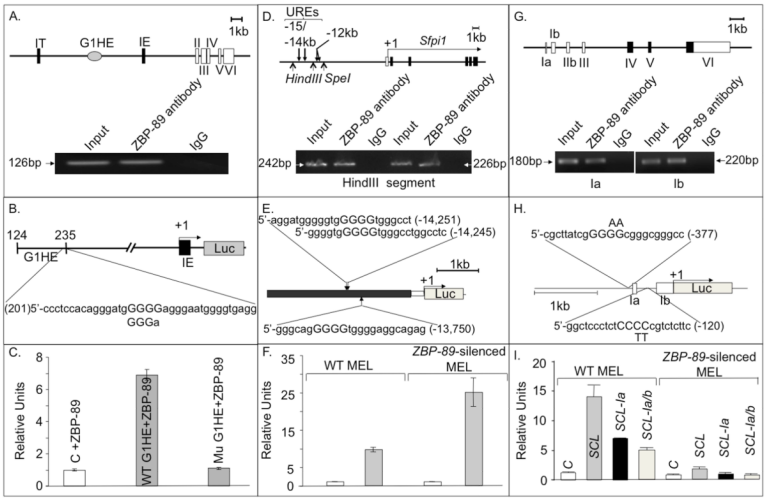

Figure 6. ZBP-89 is a transcriptional regulator of *GATA1*, *PU.1* and *SCL*

(A) Schematic of a genomic segment containing mouse *GATA1* locus, with two cell-type specific first exons (*IT* and *IE*), five coding exons (*II–VI*), and the G1HE region. The other cis-regulatory elements (double GATA, CACCC and GATA repeats) are not shown. Lower panel, ChIP assays showing specific binding of ZBP-89 to the 5′ region of the GATA1 gene hematopoietic enhancer (G1HE)(which allows GATA1 expression in erythroid lineage). (B) Wt and mutant G1HE (G1HE-(124–235)-luc in which one of the G_5 string comprising the ZBP-89 core binding motif is deleted) reporter constructs used (see methods). (C) Histograms (mean±SD, n=2) showing luciferase (Luc) activity in ZBP-89-transfected QM7 cells driven by wild-type (WT) or mutant G1HE (where the ZBP-89 site is mutated). Background luciferase activity was obtained using the control (C) promoter-less vector pGL2. (D) Schematic of a genomic segment containing the nontranslated region of *PU.1*, the minimal promoter (white bar) and the five coding exons (in black). Transcription start site (+1) and direction (horizontal arrow) are shown. Lower panel, ChIP assays showing specific interaction of ZBP-89 with two PCR products in the −15/−14 URE of PU.1. Normal IgG, used as negative control, and input DNA used as a positive control. (E) pXP-214 kb/-0.334 kb/Luc plasmid containing the 3.5kb −15/−14 URE (in black) cloned upstream of the *PU.1* minimal 0.5kb promoter (in white) driving Luc reporter (in gray). Position and sequence of the three predicted ZBP-89 binding sites (core motif capitalized) in −15/14 URE are shown. (F) Histograms (mean±SD, n=2) showing Luc activity in WT and *ZBP-89*-silenced MEL cells driven by −15/14 URE. In C, F, I, relative units represent Luc activity normalized against β-Gal values. (G) Schematic of a genomic segment containing mouse *SCL*, comprising 7 exons, with noncoding exons in white. Lower panel, ChIP assays showing specific interaction of ZBP-89 with *1a* or *1b* promoter regions. (H) Schematic of the construct containing promoters *la* and *lb* of *SCL* cloned upstream of Luc in SCL-pGL2 vector. The two predicted ZBP-89 binding sites are shown. Position and nature of substitution of the two central pyrimidines in the ZBP-89 binding motif of *la* and *lb* are indicated above and below the respective sequence. Exons *1a* and *1b* are shown as white boxes. (I) Histograms (mean ± SD, n=2) showing Luc activity driven by −2kb to +1 DNA region of WT *SCL* or by *SCL* in which ZBP-89 consensus-binding sites in promoter *1a* (*SCL-1a*) or 1a+1b (*SCL-1a/b*) were mutated. Background luciferase activity was obtained using the control promoter-less vector pGL2.

Table 1

Immunophenotype of wild-type and ZBP-89-silenced FDCP-A4 (A4) cells

Cell Lineage	Surface marker	Percent Positive Cells		P value
		A4	H5-A4	
Megakaryocytes	CD41	80.3±5.1*	55.1±11.1	0.022
Myeloid	CD11b	92.8±1.5	72.0±12.2	0.043
B cells	B220	47.9±8.1	77.2±2.2	0.004
T cells	CD3	1.6±0.7	1.5±1.9	0.99

*Numbers represent the mean ± SD of three independent experiments.